

PHASE TRANSITIONS OF POLYCRYSTALLINE [Fe(H₂O)₆](ClO₄)₃ AND [Cr(H₂O)₆](ClO₄)₃ STUDIED BY DSC

E. Mikuli^{1}, B. Grad¹, K. Zaremba¹ and S. Wróbel²*

¹Department of Chemical Physics, Faculty of Chemistry, Jagiellonian University, ul. Ingardena 3, 30-060 Cracow, Poland

²Department of Solid State Physics, M. Smoluchowski Institute of Physics, Jagiellonian University, ul. Reymonta 4, 30-059 Cracow, Poland

(Received June 16, 2003; in revised form November 19, 2003)

Abstract

Fourier transform far- and mid-infrared (FT-FIR and FT-MIR) and Fourier transform Raman scattering (FT-RS) spectra of [Fe(H₂O)₆](ClO₄)₃ and [Cr(H₂O)₆](ClO₄)₃ indicate that these compounds are ionic molecular crystals built from complex cations and complex anions of octahedral (*T_h*) and tetrahedral (*T_d*) symmetry, respectively. The thermodynamic parameters for two phase transitions in polycrystalline [Fe(H₂O)₆](ClO₄)₃ and [Cr(H₂O)₆](ClO₄)₃ were determined by differential scanning calorimetry (DSC): melting of the crystals (at *T_m*=359.2 and 363.1 K) and solid–solid phase transition (at *T_{C1}*=126.5 and 139.4 K), respectively.

Keywords: DSC, FT-IR, FT-RS, hexaaquachromium(III) chlorate(VII), hexaaquairon(III) chlorate(VII), phase transitions

Introduction

Phase transitions and their connections with the molecular motions in hexaaqua-metal(II) chlorates(VII) were widely studied by quite a lot of experimental methods and many authors ([1–3] and papers quoted therein). Unfortunately, in the literature such information is missing for a hexaaquametal(III) complexes, especially of trivalent transition metals, and furthermore there is no information about their structure and physicochemical properties. Certainly one of the reasons is that these substances are strongly hygroscopic and very easily hydrolyzed. However, there were some investigations for the aqueous acidic solutions of these salts, including: Raman [4], Mössbauer [5, 6], NMR [7, 8], ESR [9] and X-ray [10] and Incoherent Quasi-elastic Neutron [11] scattering.

The aim of this study is to detect the phase polymorphism of the title compounds and to determine the thermodynamic parameters of the detected phase transitions.

* Author for correspondence: E-mail: mikuli@chemia.uj.edu.pl

Experimental

The investigated compounds were purchased from Aldrich Company and used without further purification. Before the measurements, the composition of the compounds was determined on the basis of metal content, with titration by means of EDTA. Chemical analysis confirmed presence of hexaaquairon(III) chlorate(VII) and hexaaquachromium(III) chlorate(VII). The average contents of iron and chromium were found to be equal to the theoretical values within the error limit of ca. 3 and 4%, respectively.

The infrared absorption measurements (FT-FIR and FT-MIR) were performed with a Digilab FTS-14 and Bruker Equinox 55 Fourier transform infrared spectrometers with a resolution of 2 and 1 cm^{-1} , respectively. The FT-FIR spectra for powder samples suspended in Apiezon grease were recorded. Polyethylene and silicon windows were used. The FT-MIR spectra were recorded both for the sample suspended in Nujol oil between KBr windows and for the sample compressed in KBr pellet.

Fourier transform Raman scattering measurements (FT-RS) were performed at room temperature with a Bio-Rad spectrometer, resolution 4 cm^{-1} . The incident radiation ($\lambda=1064 \text{ nm}$) came from a Neodymium laser YAG Spectra-Physics.

The DSC measurements at 95–300 K were performed with a Perkin Elmer Pyris 1 DSC apparatus. The measurements were made both on heating and cooling of the samples at constant rates of 10, 20 and 30 K min^{-1} . The samples of $[\text{Fe}(\text{H}_2\text{O})_6](\text{ClO}_4)_3$ and $[\text{Cr}(\text{H}_2\text{O})_6](\text{ClO}_4)_3$, masses 10.81 and 11.55 mg, respectively, were placed in an aluminum vessel, mass ca. 26 mg, and closed by compressing. Another empty aluminum vessel was used as a reference holder. Two characteristic temperatures of the DSC peaks obtained on sample heating and cooling were computed: peak maximum temperature (T_{peak}) and temperature calculated from the slope of the left-hand side of the peak (T_{onset}). These two temperatures differed by 2 to 4 K, what depended on the scanning rate of heating or cooling. The enthalpy changes (ΔH) connected with the observed phase transitions were calculated by numerical integration of the DSC curves under the peaks of the anomalies. Before the calculations a linear background was subtracted. This was done in a more or less arbitrary though identical way for all peaks. The entropy changes (ΔS) were calculated using formula: $\Delta S = \Delta H / T_C$. The other experimental details were the same as published in [12].

The Mössbauer effect measurement was performed at room temperature by means of a laboratory made instrument with $^{57}\text{Co}/\text{Rh}$ source (30 mCi).

Results and discussion

Identification of the compounds

Figure 1 presents the comparison of the Raman (FT-RS) spectra and Fig. 2 the comparison of the infrared (FT-FIR and FT-MIR) spectra of $[\text{Fe}(\text{H}_2\text{O})_6](\text{ClO}_4)_3$ and $[\text{Cr}(\text{H}_2\text{O})_6](\text{ClO}_4)_3$. There are following 51 normal modes for the complex $[\text{M}(\text{H}_2\text{O})_6]^{2+}$ of T_h symmetry: $3A_g + A_u + 3E_g + E_u + 5F_g + 8F_u$ [13]. However, modes $3A_g$, $3E_g$, $5F_g$, A_u and E_u are infrared inactive and modes A_u , E_u and $8F_u$ are Raman inactive [13].

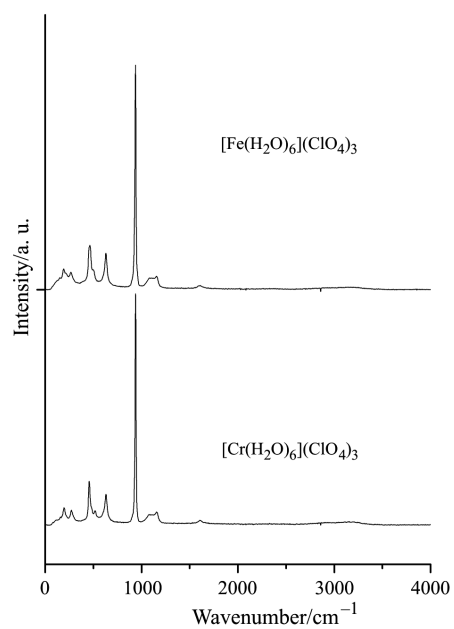


Fig. 1 Comparison of FT-RS spectra for [Cr(H₂O)₆](ClO₄)₃ and [Fe(H₂O)₆](ClO₄)₃

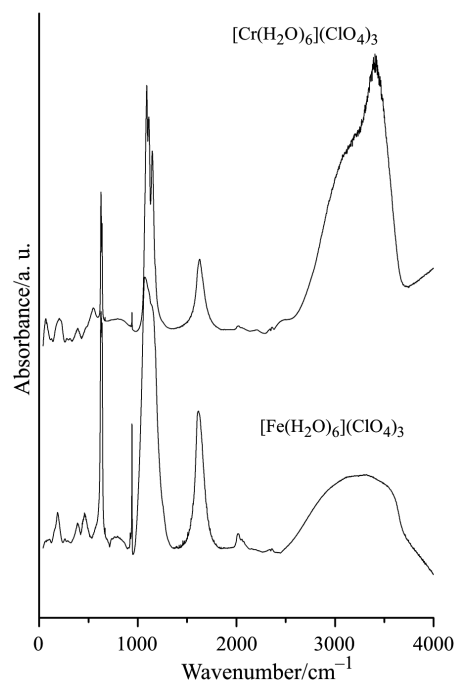


Fig. 2 Comparison of FT-IR spectra for [Cr(H₂O)₆](ClO₄)₃ and [Fe(H₂O)₆](ClO₄)₃

Tetrahedral ClO_4^- anion has nine normal modes: A_1 , E and $2F_2$ and all of them are Raman active but infrared active are only $2F_2$ [14]. The list of the band positions of the Raman and infrared spectra at room temperature, their relative intensities and their assignment for both investigated compounds are presented in Table 1. Quite a good agreement of the assignments proves the proper composition of the title compounds. The great similarity of their vibrational spectra indicates that the molecular structure and molecular dynamic of these compounds are also very similar. FT-FIR, FT-MIR, FT-RS spectra of $[\text{Fe}(\text{H}_2\text{O})_6](\text{ClO}_4)_3$ and $[\text{Cr}(\text{H}_2\text{O})_6](\text{ClO}_4)_3$ indicate that they are ionic molecular crystals built from complex cations and complex anions of the octahedral (T_h) and tetrahedral (T_d) symmetry, respectively.

The Mössbauer absorption spectrum of $[\text{Fe}(\text{H}_2\text{O})_6](\text{ClO}_4)_3$ is shown in Fig. 3. The spectrum was measured to confirm the octahedral coordination of Fe^{3+} by H_2O ligands. There are two picks on the Mössbauer spectrum, one big and broad and second one much smaller. The spectrum was decomposed by standard software into two lines, whose separation represents the presence of two kinds of iron ions: Fe^{2+} and Fe^{3+} . Big pick with its isomeric shift $\delta=0.32 \text{ mm s}^{-1}$ and quadrupole splitting $Q.S.=0.25 \text{ mm s}^{-1}$ is characteristic for Fe^{3+} low spin complexes [15, 16]. The value of $Q.S.$ suggests almost homogeneous electric field and octahedral structure of the complex cation [15, 17]. The second picks is for isomeric shift $\delta=1.13 \text{ mm s}^{-1}$ and quadrupole splitting $Q.S.=1.55 \text{ mm s}^{-1}$. It is probably present because of a pollution of sample contamination with Fe^{2+} ions [15]. Relative area under those two gives information about the percentage amount of Fe^{2+} ions, which was calculated at ca. 10%.

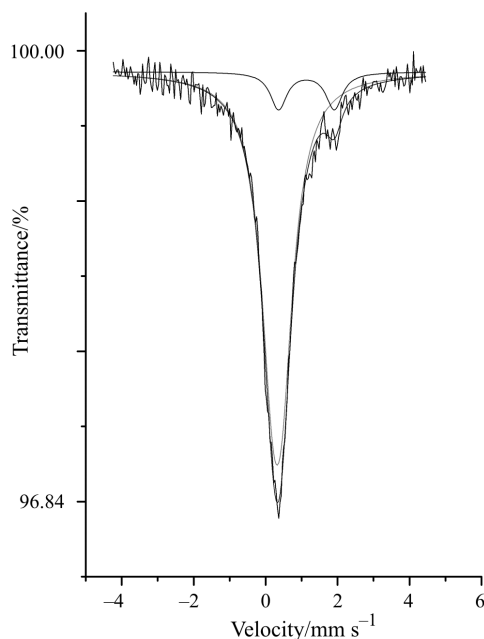


Fig. 3 Mössbauer spectrum of $[\text{Fe}(\text{H}_2\text{O})_6](\text{ClO}_4)_3$

Table 1 The list of band positions of the Raman and infrared spectra of $[\text{Fe}(\text{H}_2\text{O})_6](\text{ClO}_4)_3$ and $[\text{Cr}(\text{H}_2\text{O})_6](\text{ClO}_4)_3$ at room temperature (vw – very weak, w – weak, sh – shoulder, m – medium, st – strong, vst – very strong, br – broad) and a comparison with the literature data

$[\text{Fe}(\text{H}_2\text{O})_6](\text{ClO}_4)_3$		$[\text{Cr}(\text{H}_2\text{O})_6](\text{ClO}_4)_3$		Assignments
RS	IR	RS	IR	
?		?		$\nu_{\text{as}}(\text{OH})E_{\text{g}}$
?		?		$\nu_{\text{s}}(\text{OH})F_{\text{g}}$
	3400 br		3400 br	$\nu_{\text{as}}(\text{OH})F_{\text{u}}$
3200 vw		3200 vw		$\nu_{\text{s}}(\text{OH})A_{\text{g}}$
	3100 br		3100 br	$\nu(\text{OH})F_{\text{u}}$
	1616 st		1627 st	$\delta_{\text{as}}(\text{HOH})F_{\text{u}}$
?		?		$\delta_{\text{as}}(\text{HOH})E_{\text{g}}$
1608 w		1608 w		$\delta_{\text{as}}(\text{HOH})A_{\text{g}}$
1140 m	1148 vst	1140 m	1147 vst	
	1111 vst		1112 vst	$\nu_{\text{d}}(\text{ClO})F_2$
1088 m	1088 vst	1083 m	1090 vst	
941 vst	940 st	942 vst	940 st	$\nu_{\text{s}}(\text{ClO})A_1$
?		?		$\rho_{\text{r}}(\text{H}_2\text{O})F_{\text{g}}$
	800 w		800 w	$\rho_{\text{r}}(\text{H}_2\text{O})F_{\text{u}}$
	633 sh		634 sh	
635 st	628 st	633 st	628 st	$\delta_{\text{d}}(\text{OClO})F_2$
	625 vst		625 vst	
	507 m		551 m	$\rho_{\text{w}}(\text{H}_2\text{O})F_{\text{u}}$
507 sh		520 sh		$\rho_{\text{w}}(\text{H}_2\text{O})F_{\text{g}}$
?		?		$\rho_{\text{t}}(\text{H}_2\text{O})F_{\text{g}}$
466 st		464 st		$\delta_{\text{d}}(\text{OClO})E$
	394 st		391 st	$\nu_{\text{as}}(\text{FeO})F_{\text{u}}$ $\nu_{\text{as}}(\text{CrO})F_{\text{u}}$
	292 vw		319 w	
?		?		$\nu_{\text{s}}(\text{FeO})E_{\text{g}}$ $\nu_{\text{s}}(\text{CrO})E_{\text{g}}$
274 m		275 m		$\nu_{\text{s}}(\text{FeO})A_{\text{g}}$ $\nu_{\text{s}}(\text{CrO})A_{\text{g}}$
	262 m		287 w	$\delta(\text{OFeO})F_{\text{u}}$ $\delta(\text{OCrO})F_{\text{u}}$
	188 st		204 st	$\delta(\text{OFeO})F_{\text{u}}$ $\delta(\text{OCrO})F_{\text{u}}$
191 m		199 m		$\delta(\text{OFeO})F_{\text{g}}$ $\delta(\text{OCrO})F_{\text{g}}$
	108 m		126 m	$\nu_{\text{l}}(\text{lattice})$
70 vw	93 vw	70 vw	92 vw	$\nu_{\text{l}}(\text{lattice})$
50 vw	81 br	50 vw	67 st	$\nu_{\text{l}}(\text{lattice})$

DSC investigations

Figure 4 presents the temperature dependence of the heat flow (DSC curve) obtained on heating of the $[\text{Cr}(\text{H}_2\text{O})_6](\text{ClO}_4)_3$ sample at the rate of 30 K min^{-1} . Two anomalies on the DSC curve were registered: one very small at $T_{\text{peakl}}^{\text{h}} = 140.58 \text{ K}$, connected with the solid-state phase transition and one very big at $T_{\text{peakm}}^{\text{h}} = 363.1 \text{ K}$, connected with the melting of the compound. The solid-state phase transition temperatures: $T_1^{\text{h}} = 139.67 \text{ K}$ (on heating) and at $T_1^{\text{c}} = 139.06 \text{ K}$ (on cooling) were calculated by extrapolating the dependences of $T_{\text{peak}}^{\text{h}}$ and $T_{\text{peak}}^{\text{c}}$ vs. the rate of sample heating and cooling to the scanning rate value of 0 K min^{-1} . The presence of ca. 0.6 K hysteresis in the phase transition temperature and the sharpness of the heat flow anomaly suggest that the detected phase transition is of the first-order type. The thermodynamic parameters of the detected phase transitions are presented in Table 2.

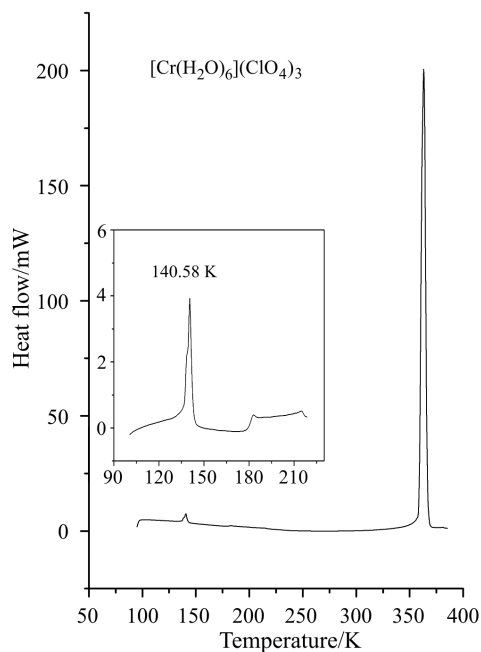


Fig. 4 DSC curve of $[\text{Cr}(\text{H}_2\text{O})_6](\text{ClO}_4)_3$ obtained at a heating constant rate of 30 K min^{-1}

Figure 5 presents the temperature dependence of the heat flow (DSC curve) obtained on heating of the $[\text{Fe}(\text{H}_2\text{O})_6](\text{ClO}_4)_3$ sample at the rate of 30 K min^{-1} . Two anomalies on the DSC curve were registered: one very small at $T_{\text{peakl}}^{\text{h}} = 128.16 \text{ K}$, connected with the solid-state phase transition and one very big at $T_{\text{peakm}}^{\text{h}} = 359.2 \text{ K}$, connected with the melting of the compound. The solid-state phase transition

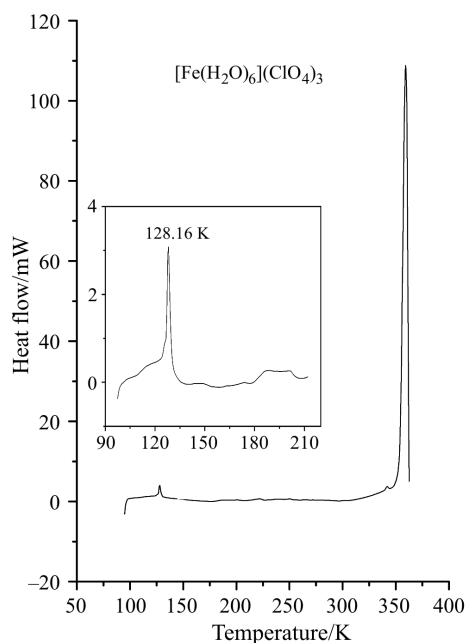


Fig. 5 DSC curves of $[\text{Fe}(\text{H}_2\text{O})_6](\text{ClO}_4)_3$ obtained at a heating constant rate of 30 K min^{-1}

temperatures: $T_1^{\text{h}} = 126.82 \text{ K}$ (on heating) and $T_1^{\text{c}} = 126.31 \text{ K}$ (on cooling) were calculated by extrapolating the dependences of $T_{\text{peak}}^{\text{h}}$ and $T_{\text{peak}}^{\text{c}}$ vs. the rate of sample heating and cooling to the scanning rate value of 0 K min^{-1} . The presence of ca. 0.5 K hysteresis in the phase transition temperature and the sharpness of the heat flow anomaly suggest that the detected phase transition is of the first-order type. The thermodynamic parameters of the detected phase transitions are presented in Table 2.

Table 2 Mean values of the thermodynamic parameters of the phase transitions in $[\text{Fe}(\text{H}_2\text{O})_6](\text{ClO}_4)_3$ and $[\text{Cr}(\text{H}_2\text{O})_6](\text{ClO}_4)_3$

	$[\text{Fe}(\text{H}_2\text{O})_6](\text{ClO}_4)_3$	$[\text{Cr}(\text{H}_2\text{O})_6](\text{ClO}_4)_3$
T_{melt}/K	359.2 ± 0.1	363.1 ± 0.1
$\Delta H/\text{kJ mol}^{-1}$	51.8 ± 3.0	75.7 ± 4.1
$\Delta S/\text{J mol}^{-1} \text{ K}^{-1}$	144.0 ± 8.0	208.4 ± 9.5
T_{C1}/K	126.5 ± 0.2	139.4 ± 0.4
$\Delta H/\text{kJ mol}^{-1}$	0.5 ± 0.1	0.6 ± 0.1
$\Delta S/\text{J mol}^{-1} \text{ K}^{-1}$	4.1 ± 0.3	4.6 ± 0.4

The great similarity of the phase transition parameters for the both investigated compounds confirm both their similar molecular structure and molecular dynamics.

Conclusions

1. Two phase transitions and their thermodynamic parameters were determined for polycrystalline $[\text{Fe}(\text{H}_2\text{O})_6](\text{ClO}_4)_3$ and $[\text{Cr}(\text{H}_2\text{O})_6](\text{ClO}_4)_3$:
 - Melting of these crystals at T_m equal to 359.2 and 363.1 K, respectively;
 - Solid–solid phase transition at T_{C1} equal to 126.5 and 139.4 K, respectively.
2. Vibrational spectra of $[\text{Fe}(\text{H}_2\text{O})_6](\text{ClO}_4)_3$ and $[\text{Cr}(\text{H}_2\text{O})_6](\text{ClO}_4)_3$ are characteristic of ionic molecular crystals built from octahedral (T_h) complex cations and tetrahedral (T_d) complex anions.
3. The great similarity of the vibrational spectra and the phase transition parameters for the both investigated compounds confirm their similar molecular structure and molecular dynamics.

* * *

We would like to thank Professor J. Stanek from M. Smoluchowski Institute of Physics of the Jagiellonian University for the Mössbauer measurement. We are also grateful to Dr. A. Weselucha-Birczyńska from the Regional Laboratory of Physicochemical Analysis and Structural Research in Cracow, J. Ściesiński M.Sc. and Dr. hab. E. Ściesińska from the Institute of Nuclear Physics in Cracow and M. Jakus M.Sc. from our Faculty for FT-RS, FT-FIR and FT-MIR measurement, respectively.

References

- 1 E. Mikuli, A. Migdał-Mikuli and J. Mayer, *J. Therm. Anal. Cal.*, 54 (1998) 93.
- 2 E. Mikuli, A. Migdał-Mikuli, I. Natkaniec and B. Grad, *Z. Naturforsch.*, 56a (2000) 244.
- 3 C. Nöldeke, B. Asmussen, W. Press, H. Büttner and G. Kearley, *Chem. Phys.*, 289 (2003) 275.
- 4 S. K. Sharma, *J. Inorg. Nucl. Chem.*, 35 (1973) 3831.
- 5 J. W. G. Wignall, *J. Chem. Phys.*, 44 (1965) 2462.
- 6 S. Mørup, J. E. Kundsén, M. K. Nielsen and G. Trumpy, *J. Chem. Phys.*, 65 (1976) 536.
- 7 B. B. Wayland and W. L. Rice, *Inorg. Chem.*, 5 (1966) 54.
- 8 I. Bertini, F. Capozzi, C. Luchinat and Z. Xia, *J. Phys. Chem.*, 97 (1993) 1134.
- 9 H. Levanon, H. Charbinsky and Z. Luz, *J. Chem. Phys.*, 53 (1970) 3056.
- 10 M. Magini, *J. Inorg. Nucl. Chem.*, 40 (1978) 43.
- 11 P. S. Salmon, G. J. Herdman, J. Lindgren, M. C. Read and M. Sandström, *J. Phys.: Condens. Matter*, 1 (1989) 3459.
- 12 A. Migdał-Mikuli, E. Mikuli, S. Wróbel, Ł. Hetmańczyk, *Z. Naturforsch.*, 54a (1999) 590.
- 13 I. Nakagawa, T. Shimanouchi, *Spectrochim. Acta*, 20 (1964) 429.
- 14 K. Nakamoto, *Infrared and Raman Spectra of Inorganic and Coordination Compounds*, 5th Ed., Wiley, New York 1997.
- 15 P. Gülich, R. Link and A. Trautwien, *Mössbauer Spectroscopy and Transition Metal Chemistry*, Springer, Berlin 1978.
- 16 B. Papánková, M. Vrbová, R. Bača, P. Šimon, K. Falk, G. Miehe and H. Fuess, *J. Therm. Anal. Cal.*, 67 (2002) 721.
- 17 A. Vértes, L. Korecz and K. Burger, *Mössbauer Spectroscopy*, Akadémiai K., Budapest 1979.